JOURNAL OF SOLID STATE CHEMISTRY 65, 118–126 (1986)

Crystal Structure and Topotactic Dehydration of Magnesium Tungstate Dihydrate, $MgWO_4 \cdot 2H_2O$

JOHN R. GÜNTER* AND ERICH DUBLER

Institute for Inorganic Chemistry, University of Zürich, Winterthurerstrasse 190, CH-8057 Zürich, Switzerland

Received February 3, 1986; in revised form March 17, 1986

$MgWO_4 \cdot 2H_2O$ crystallizes in the monoclinic space group $P2_1/c$, $a = 5.917(1)$, $b = 10.243(2)$, $c = 8.566(1)$ Å, $\beta = 90.05(2)°$. Its crystal structure consists of individual layers built up from edge-sharing pairs of $MgO_4(H_2O)_2$ octahedra corner linked with WO_4 tetrahedra. Thermal dehydration leads in a first topotactic step to monoclinic (eventually triclinic) $MgWO_4 \cdot H_2O$, for which a structural model has been deduced, based on its unit cell ($a = 9.246$, $b = 10.773$, $c = 8.564$ Å, $\gamma = 92.43°$) and the relative orientation relations between the two lattices. It corresponds to a so far unobserved atomic arrangement, predicted to exist by earlier authors on theoretical grounds. The loss of the remaining water is again topotactic, but leads to a multiply twinned product, which corresponds in its powder diffraction pattern closely to high-temperature $MgWO_4$, reported to exist above 1200°C only, and is transformed into the stable wolframite structure at 650°C. These observations are attributed to the topotactic nature of the dehydration process.

Introduction

Although a considerable number of compounds in the system magnesium/tungstate/water have been reported in literature, structural data in this field are scarce. The following solids have been characterized:

Hydrates. $MgWO_4 \cdot 5H_2O$ (*1*), unindexed X-ray powder diffraction pattern, $MgWO_4 \cdot 2H_2O$ (*1, 2*), hexagonal unit cell reported, $MgWO_4 \cdot H_2O$ (*1, 2*), powder pattern unindexed, $MgWO_4 \cdot 7H_2O$ (*3*) and $MgWO_4 \cdot 3H_2O$ (*4*) in literature of the 19th century and not reproduced since;

Polytungstates. $MgO \cdot 2WO_3 \cdot 6H_2O$ and $5MgO \cdot 12WO_3 \cdot 43H_2O$ (*5*), with only the strongest X-ray diffraction lines indicated (the latter compound most probably corresponds to magnesium paratungstate, $Mg_5H_2W_{12}O_{42} \cdot 38H_2O$, the crystal structure of which has been determined (*6*)); one cubic and two trigonal forms of magnesium heteropolytungstates, the crystal structures of which are presently being solved (*7, 8*), the cubic phase corresponding to the compound formerly described as cubic $MgWO_4$ (*9*);

Anhydrous $MgWO_4$. The stable form at low temperature belongs to the monoclinic wolframite structure type (*10, 11*). At about 1200°C, it transforms reversibly into a high-temperature modification with unknown structure (*1, 9, 12–14*), the powder pattern of which has been reported (*13*). If prepared from hydrated precursors, another form has been reproducibly observed (*1, 2, 9, 14*), which is very similar to the high-

* To whom correspondence should be addressed.

0022-4596/86 $3.00

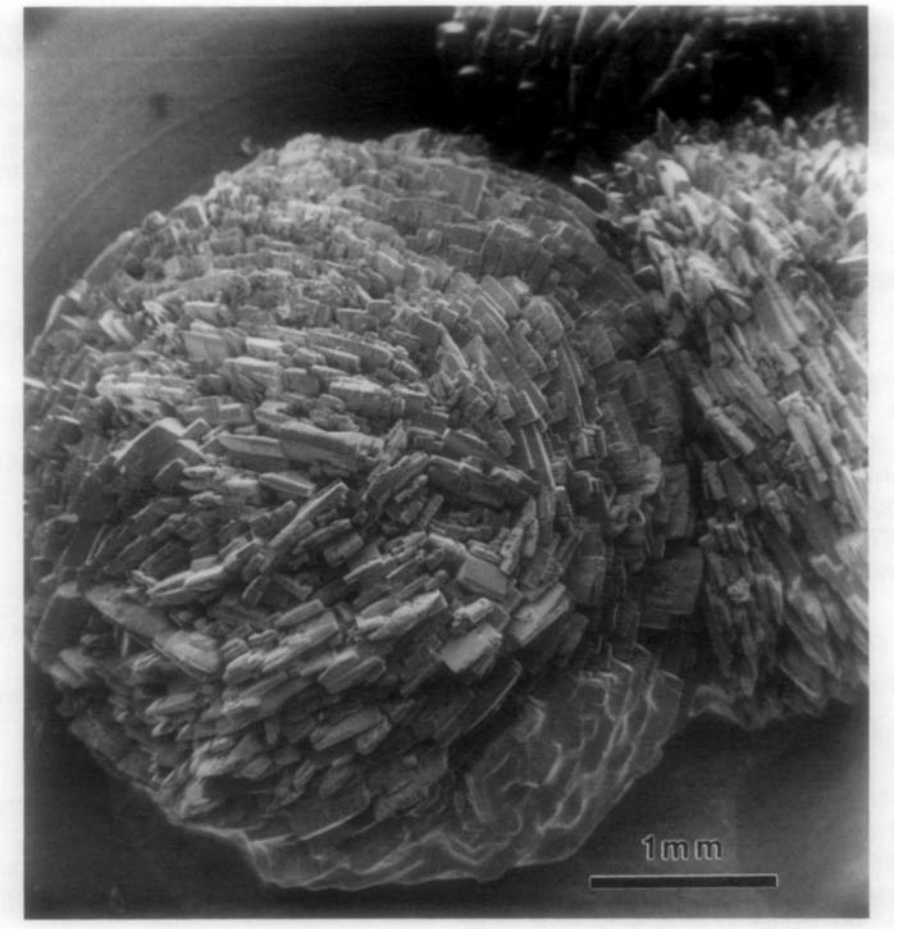

FIG. 1. Scanning electron micrograph of a hemispherical aggregate of $MgWO_4 \cdot 2H_2O$ crystals.

temperature phase, but has fewer and broader diffraction lines. In analogy to a potassium tungstate, it has been assigned tetragonal symmetry (*1*). It is transformed into the wolframite type below 800°C. The cubic form reported in (*9*) has been shown to be a polytungstate (*7*), and the existence of Mg_2WO_5 (*12*) was later disproved (*14*).

Experiments aimed at preparing magnesium heteropolytungstates (*7, 8*) yielded single-crystalline magnesium tungstate dihydrate as a byproduct. The present paper deals with its crystal structure and topotactic dehydration behavior.

Experimental

Equal volumes of 1 *M* solutions of magnesium chloride and of sodium tungstate were mixed at room temperature, sealed in pyrex tubes filled to 90–95% and stored at 90°C for one to several weeks. The glass walls were then found to be covered with a white layer of crystals of three distinct morphologies. Rhombic dodecahedra and needles with a hexagonal cross section proved to be cubic and trigonal heteropolytungstates, respectively, while large hemispherical crystal aggregates of 1 to 5 mm in diam-

eter (Fig. 1) were identified by X-ray powder diffraction as $MgWO_4 \cdot 2H_2O$. All three species were proved by energy dispersive X-ray spectroscopy to contain no other heavy elements ($Z \geq 11$) than magnesium and tungsten. Crystals for X-ray structure analysis of the dihydrate were cleaved from the hemispherical aggregates by slight crushing.

X-ray powder diffraction patterns of $MgWO_4 \cdot 2H_2O$ are in good agreement with published data (*2*), but single-crystal precession and Weissenberg photographs clearly reveal that its true symmetry is not hexagonal, but monoclinic pseudo-orthorhombic. Table I compares the hexagonal indexing from (*2*) with the new monoclinic indexing.

TABLE I

X-RAY POWDER DIFFRACTION PATTERN OF $MgWO_4 \cdot 2H_2O$[a]

Hexagonal (2) a = 11.78 Å, c = 8.606 Å			Monoclinic (this work) a = 5.917 Å, b = 10.243 Å, c = 8.566 Å, β = 90.05° Space group $P2_1/c$		
d	I/I_0	$h\,k\,l$	$d_{obs.}$	I/I_0	$h\,k\,l$
6.531	3	1 0 1	6.604	4	0 1 1
5.89	35	1 1 0	5.942	18	1 0 0
5.10	100	2 0 0	5.138	100	1 1 0 / 0 2 0
4.28	8	0 0 2	4.299	39	0 0 2
3.518	10	2 1 1	3.542	39	1 2 1
			3.484	2	1 0 2
3.279	65	2 0 2	3.301	95	1 1 2 / 0 2 2
3.164	10	3 0 1	3.185	45	0 3 1
2.951	30	2 2 0	2.967	52	2 0 0 / 1 3 0
			2.883	9	1 2 2
2.830	20	3 1 0	2.854	30	2 1 0
			2.806	7	1 3 1
			2.762	10	0 1 3
2.681	2	3 1 1	2.709	4	2 1 1
2.556	25	4 0 0	2.569	30	2 2 0 / 0 4 0
			2.500	3	1 1 3 / 0 2 3
2.423	13	2 2 2	2.443	43	2 0 2 / 1 3 2
2.361	5	3 1 2	2.377	9	2 1 2
2.256	3	3 2 1	2.275	39	1 4 1
2.191	8	4 0 2 / 3 0 3	2.200	39	2 2 2 / 0 4 2
			2.171	7	2 3 1
2.149	3	0 0 4	2.149	33	0 0 4
1.984	7	2 0 4 / 5 0 1	2.000	38	0 5 1
1.969	10	3 3 0	1.984	59	2 3 2
1.923	5	4 2 0	1.943	9	3 1 0 / 2 4 0
1.880	3	2 1 4 / 4 2 1	1.894	10	3 1 1 / 2 4 1 / 1 5 1
1.833	5	5 1 0	1.847	9	3 2 0
1.807	5	3 2 3	1.821	24	1 4 3 / 0 3 4
1.790	2	5 1 1	1.796	13	3 2 1 / 3 0 2
1.784	3	3 3 2	1.770	35	3 1 2 / 2 4 2 / 1 5 2
1.756	7	4 1 3	1.767	35	2 3 3
1.725	3	0 0 5	1.741	31	2 0 4 / 1 3 4
1.701	3	6 0 0	1.715	9	2 1 4
1.684	2	4 3 0 / 5 1 2	1.696	6	3 2 2 / 0 1 5
			1.681	3	3 3 1 / 0 6 1
1.665	2	5 0 3	1.670	18	0 5 3
1.658	2	1 1 5	1.658	12	2 5 1
1.646	3	4 3 1 / 4 0 4	1.647	24	2 2 4 / 0 4 4
1.640	3	5 2 0	1.616	29	1 6 1
1.604	3	5 2 1	1.608	13	3 1 3 / 2 4 3
1.600	2	4 2 3	1.591	6	3 3 2 / 0 6 2
1.579	2	6 0 2	1.572	7	2 5 2 / 1 2 5
1.556	1	6 1 0	1.553	4	3 2 3 / 2 3 4
1.541	1	5 1 3	1.536	11	1 6 2

[a] Comparison of the hexagonally indexed pattern reported in (*2*) and the results of this work (pseudo-orthorhombic indexing with a monoclinic unit cell, oblique angle almost equal to 90°) (observed values).

Crystal Structure Determination

A single crystal with approximate dimensions 0.1 × 0.1 × 0.1 mm^3 was mounted on an Enraf-Nonius CAD-4 diffractometer. Lattice parameters of the monoclinic cell and crystal orientation were obtained from the least-squares refinement of 25 reflections in the range $12.2 \leq \theta \leq 19.8°$. The monoclinic angle β refined to 90.00° within the limits of about three standard deviations, but subsequent intensity data collection proved that the orthorhombic symmetry has to be considered as a pseudo-symmetry, since most of the *hkl* reflections exhibit intensities significantly different from those of the corresponding $hk - l$ reflections. The systematic absences $0k0$, k = odd, and $h0l$, l = odd, uniquely indicated space group $P2_1/c$. Refined crystal data are a = 5.917(1), b = 10.243(2), c = 8.566(1) Å, β = 90.05(2)°, V = 519.2 Å^3, Z = 4, d_{calc} = 3.94 g cm^{-3}, μ = 228.0 cm^{-1}. Intensity data were collected up to 2θ = 85° with the $\omega - 2\theta$ scan mode using graphite monochromated Mo$K\alpha$ radiation (h: 0 to +11, k: 0 to +19, l: −16 to +16). The maximum time limit for a final scan was 60 sec. Six standard reflections chosen to lie in dif-

TABLE II

POSITIONAL AND ISOTROPIC THERMAL PARAMETERS[a] FOR $MgWO_4 \cdot 2H_2O$

Atom	x	y	z	B(Å^2)
W	0.29456(6)	0.21469(3)	−0.00091(4)	1.096(4)
Mg	0.5248(7)	0.5020(4)	0.1853(4)	1.42(5)
O1	0.322(2)	0.3558(8)	0.6855(9)	1.8(1)
O2	0.438(2)	0.3835(8)	0.365(1)	2.0(1)
O3	−0.005(2)	0.721(1)	0.548(1)	3.4(2)
O4	0.414(2)	0.3789(8)	0.009(1)	2.9(2)
O5	0.160(2)	0.905(1)	0.314(1)	2.5(2)
O6	0.210(2)	0.590(1)	0.216(2)	3.3(2)

[a] Anisotropically refined atoms are given in the form of the isotropic equivalent thermal parameter defined as $\frac{4}{3} * [a^{2*}\beta_{11} + b^{2*}\beta_{22} + c^{2*}\beta_{33} + ac(\cos\beta)^*\beta_{13}]$.

ferent regions of reciprocal space were monitored periodically and showed no significant variation of their intensities. The intensities were reduced to F_o by correcting for Lorentz and polarization effects. Since the indices of the crystal faces of the rather small crystal could not be deduced with certainty, a spherical absorption correction ($\mu R = 2.28$) was applied. The minimum transmission factor was 5.2%, the maximum value 10.0%. Of a total of 4291 reflections measured (including standards) 3725 remained after averaging equivalent reflections (R_{int} based on $F = 0.014$ for 244 observed hkl reflections). 2518 reflections with $I > 3\sigma(I)$ finally were used for the structure determination. The position of the tungsten atoms could be deduced from a Patterson synthesis. Structure factor calculations based only on these heavy atoms resulted in a conventional R index of 0.15. Subsequent difference Fourier syntheses revealed the positions of the magnesium and oxygen atoms. The structure was refined with full-matrix least-squares methods including anisotropic temperature coefficients for all atoms and a correction for secondary extinction effects ($g = 6.9(4) \times 10^{-7}$). Final values of R and R_w are 0.066 and 0.078, respectively, on F, including 2518 observed reflections (74 variables); the goodness-of-fit S is 2.59. The function minimized was $\Sigma w(|F_o| - |F_c|)^2$ with $w = 1/[\sigma^2(F) + 0.0004F^2]$. A final difference Fourier map revealed two unusually high peaks in a distance of about 0.5 Å from the tungsten atom. In view of the very large absorption coefficient of the compound, these peaks most probably are a consequence of uncorrected absorption effects. All calculations were performed with the Enraf-Nonius program package SDP (*15*).

Atomic and isotropic thermal parameters are given in Table II. Lists of observed and calculated structure factors and a table of anisotropic thermal parameters can be obtained as supplementary deposited material.[1]

Description of Crystal Structure

The crystal structure of $MgWO_4 \cdot 2H_2O$ is distinctly layered parallel to (100), the individual layers being built up from $MgO_4(H_2O)_2$ octahedra and WO_4 tetrahedra linked with each other (Figs. 2a and b). The WO_4 tetrahedra are only slightly distorted with a mean W–O distance of 1.773 Å. This value coincides with the distance of 1.78 Å found in $CsLiWO_4$, one of the rare tetrahedral tungstates whose crystal structure has been solved (*16*). Although the MgO_6 octahedron contains four tungstate oxygen atoms and only two water molecules, the mean Mg–O distance of 2.072 Å perfectly lies within the range of 2.053–2.087 Å recently tabulated for a series of highly re-

[1] See NAPS documented No. 04391 for 14 pages of supplementary material. Order from NAPS c/o Microfiche Publications, P.O. Box 3513, Grand Central Station, New York, N.Y. 10163. Remit in advance in U.S. funds only $7.75 for photocopies or $4.00 for microfiche. Outside the U.S. and Canada, add postage of $4.50 for the first 20 pages and $1.00 for each of 10 pages of material thereafter, $1.50 for microfiche postage.

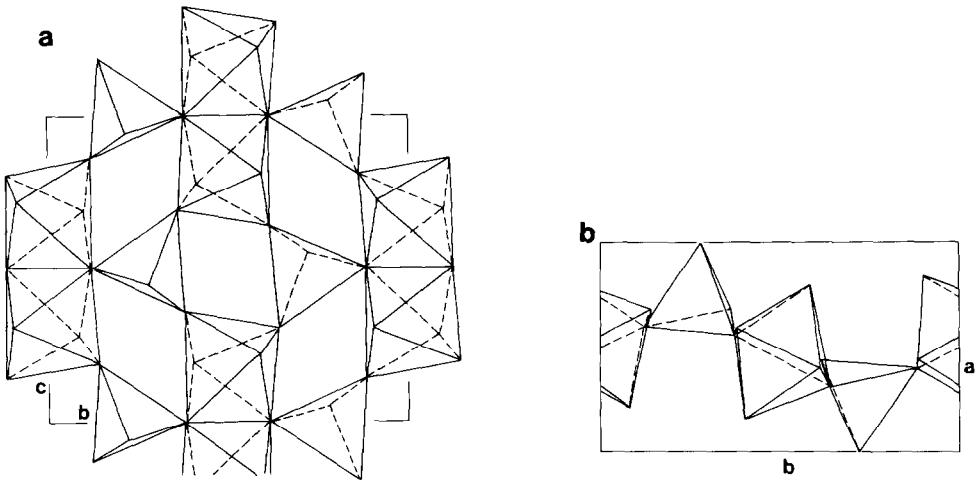

FIG. 2. (a) Projection (100) of a $MgWO_4 \cdot 2H_2O$ layer. (b) Projection (001) of half the unit cell content of $MgWO_4 \cdot 2H_2O$.

fined isolated $Mg(H_2O)_6$ octahedra (*17*). Pairs of these octahedra share O–O edges, leaving the water molecules in terminal nonbridging positions. These pairs of octahedra are connected with the tetrahedra by corner sharing in such a way that each tetrahedron has one corner in common with a bridging corner of a pair of octahedra, two corners with nonbridging corners of pairs of octahedra, and one terminal corner pointing up or down in the *a* direction in alternating rows parallel to *c*. These layers are corrugated by tilting the pairs of octahedra, essentially by about 25° in opposite direction around the *c* axis. They are stacked in identical positions above each other along *a*. A summary of interatomic bond lengths and bond angles is given in Table III.

This crystal structure, is very similar to the one of $ZnMoO_4 \cdot 2H_2O$ and $MgMoO_4 \cdot 2H_2O$ (*21*), but differs from it in symmetry (space group $P2_1/c$ instead of $P2_1$). Nevertheless, both kinds of structure correspond to type 3*a* in the classification of $MM'O_4 \cdot 2H_2O$ structures deduced by Bars *et al.* (*22*).

TABLE III

INTERATOMIC BOND DISTANCES (Å) AND BOND ANGLES (°) FOR $MgWO_4 \cdot 2H_2O$

WO_4 tetrahedron and MgO_6 octahedron			
W–O(1)	1.760(5)	O(1)–W–O(2)	108.4(3)
W–O(2)	1.746(5)	O(1)–W–O(3)	108.0(3)
W–O(3)	1.759(7)	O(1)–W–O(4)	107.5(3)
W–O(4)	1.827(5)	O(2)–W–O(3)	110.1(3)
		O(2)–W–O(4)	111.9(3)
		O(3)–W–O(4)	110.8(4)
Mg–O(1)	2.042(6)	O(1)–Mg–O(2)	97.4(2)
Mg–O(2)	2.027(5)	O(1)–Mg–O(4)	165.7(3)
Mg–O(4)	2.074(6)	O(1)–Mg–O(4′)	86.5(2)
Mg–O(4′)	2.094(7)	O(1)–Mg–O(5)	86.7(3)
Mg–O(5)	2.112(7)	O(1)–Mg–O(6)	91.2(3)
Mg–O(6)	2.084(8)	O(2)–Mg–O(4)	96.3(3)
		O(2)–Mg–O(4′)	174.9(3)
O(2)–Mg–O(5)	86.6(3)	O(4)–Mg–O(6)	94.1(3)
O(2)–Mg–O(6)	86.4(3)	O(4′)–Mg–O(5)	97.0(3)
O(4)–Mg–O(4′)	80.2(2)	O(4′)–Mg–O(6)	90.1(3)
O(4)–Mg–O(5)	89.7(3)	O(5)–Mg–O(6)	172.4(3)
Shortest metal-to-metal distances[a]			
W(I)–W(II)	5.025(0)	W(I)–Mg(V)	3.472(2)
W(I)–W(III)	4.344(0)	W(I)–Mg(III)	3.743(2)
W(I)–W(IV)	4.344(0)	W(I) Mg(VI)	3.633(2)
W(I)–Mg(I)	3.614(2)	Mg(I)–Mg(V)	3.188(5)

[a] Symmetry codes: I = x, y, z; II = $1-x, -y, -z$; III = $x, \frac{1}{2}-y, \frac{1}{2}+z-1$; IV = $x, \frac{1}{2}-y, \frac{1}{2}+z$; V = $1-x, 1-y, -z$; VI = $1-x, \frac{1}{2}+y-1, \frac{1}{2}-z$.

TABLE IV

X-RAY POWDER DIFFRACTION PATTERN OF $MgWO_4 \cdot H_2O$[a]

$d_{obs.}$	I/I_0	$h\ k\ l$
6.627	4	0 1 1
5.483	35	$\bar{1}$ 1 1
4.805	18	$\bar{1}$ 2 0
4.619	55	2 0 0
4.548	50	1 2 0
3.897	50	1 0 2
3.847	45	$\bar{2}$ 1 1
3.728	8	2 1 1
3.348	100	0 2 2
3.324	100	0 3 1
3.178	11	$\bar{1}$ 2 2
2.833	20	$\bar{3}$ 1 1
2.773	34	3 1 1
2.748	38	0 1 3 / $\bar{2}$ 2 2
2.696	22	0 4 0
2.646	8	2 3 1 / $\bar{1}$ 1 3 / 1 1 3
2.605	8	$\bar{1}$ 4 0
2.523	1	0 2 3
2.363	7	$\bar{2}$ 4 0
2.336	6	2 1 3
2.277	7	0 4 2
2.228	4	0 3 3
2.187	4	$\bar{1}$ 3 3
2.130	3	0 0 4
2.088	4	0 5 1
2.079	4	$\bar{3}$ 4 0
2.021	4	1 5 1
1.947	15	$\bar{1}$ 2 4 / 2 0 4
1.806	2	3 4 2
1.779	4	$\bar{4}$ 1 3
1.729	4	5 2 0

[a] Monoclinic: $a = 9.246$ Å, $b = 10.773$ Å, $c = 8.564$ Å, $\gamma = 92.43°$.

Thermal Dehydration

Thermogravimetric results are in good agreement with (*1, 2*), showing the water loss to occur in two distinct equal steps, starting at 100 and 150°C respectively under dynamic conditions (10°/min in air). The intermediate monohydrate appears to be stable between about 120 and 150°C. These results have also been confirmed by continuous high temperature X-ray powder diffraction, proving that the loss of one water molecule per formula unit leads to $MgWO_4 \cdot H_2O$ as reported in (*1, 2*) and the loss of the remaining water to a poorly crystallized phase, the diffraction pattern of which closely corresponds to that of high temperature $MgWO_4$ (*13*; see below). To obtain more information on the two decomposition products, crystals were partly or completely dehydrated by isothermal treatment at various temperatures and then subjected to single crystal X-ray diffraction (precession and Weissenberg techniques). This proved both steps of the reaction to be topotactic in nature, the pseudomorphs yielding diffraction patterns with distinct spots in reproducible arrangements. We have shown previously (*18, 19*) that the knowledge of the initial crystal structure, the topotactic orientation relations and the unit cell of the product can be used to deduce the principle atomic arrangements in unknown product structures. The same line of arguments will now be used to derive a model structure for $MgWO_4 \cdot H_2O$. Some observations on the thermal behavior of the anhydrous product obtained will finally be reported.

Magnesium Tungstate Monohydrate

Precession photographs of crystals dehydrated partly or completely to the monohydrate by heating in air for several hours at temperatures between 110 and 130°C yielded a unit cell, with which the X-ray powder diffraction pattern of $MgWO_4 \cdot H_2O$ could be indexed (Table IV), as well as its relative orientation to the parent dihydrate. The unit cell obtained by least-squares refinement of the powder diffraction data is monoclinic, with $a = 9.246$, $b = 10.773$, $c = 8.564$ Å and $\gamma = 92.43°$, with pronounced twinning on (100). The topotactic orientation relations between the two hydrates are

a_{mono} (9.246 Å) parallel to a_{di} (5.917 Å) $\mp$ 2.5°,

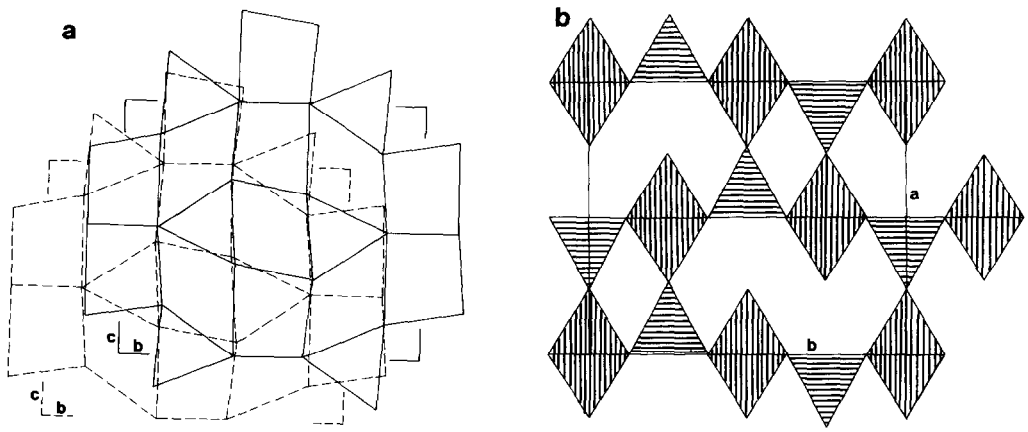

FIG. 3. (a) Projection (100) of the $MgWO_4 \cdot H_2O$ model structure, one layer being shifted by $b/4 + c/4$ relative to the other. Terminal corners omitted for clarity. The superposition of octahedra of one layer with tetrahedra of the neighboring layer, completing the Mg coordination after loss of water is evident. (b) Projection (001) of $MgWO_4 \cdot H_2O$ model structure; corrugation of the layers is not shown, as its extent is not known exactly. $MgO_5(H_2O)$ octahedra are shaded vertically; WO_4 tetrahedra, horizontally.

b_{mono} (10.773 Å) parallel to b_{di} (10.243 Å), c_{mono} (8.564 Å) parallel to c_{di} (8.566 Å).

This orientation implies that the oblique angle γ of the monoclinic cell of the monohydrate is not the same as the monoclinic angle β of the dihydrate, possibly indicating that the true symmetry of the monohydrate is triclinic pseudo-monoclinic.

Comparison of the unit cells in their experimentally found relative orientation shows that the layers (100) change their dimensions only slightly (+5% in b and −0.02% in c) and at the same time conserve their orientation, indicating that the first step of dehydration is a topotactic process controlled by the conservation of layers (*20*). The a axis, however, is shortened by about 22% and at the same time doubled, implying a change in the stacking sequence of the layers. From these observations, the following model structure for $MgWO_4 \cdot H_2O$ has been deduced.

The essentially unaltered but less corrugated layers of the dihydrate, after loss of half of the water molecules, are stacked in such a way that every other layer is shifted by $b/4$ and $c/4$, bringing the terminal corners of WO_4 tetrahedra near to the positions formerly occupied by water coordinated to magnesium. Approaching these layers parallel to a and deforming them only slightly recompletes the magnesium coordination octahedra to $MgO_5(H_2O)$ and produces the arrangement shown in Figs. 3a and b, having the unit cell dimensions determined for the monohydrate. The structure does not show the character of a layered arrangement any more, but rather that of a three-dimensional lattice, containing the crystal water coordinated to Mg in channels running parallel to c. This model structure derived from topotaxy data is indeed the first representative of a structural type deduced theoretically in a systematic study on possible atomic arrangements for $MM'O_4 \cdot H_2O$ compounds by Bars *et al.* (*23*) and named type 1 by these authors.

Anhydrous Magnesium Tungstate

Crystals dehydrated at temperatures above 150°C yield precession photographs still showing defined, though broadened reflections instead of powder diffraction rings

TABLE V

X-RAY POWDER DIFFRACTION PATTERN OF ANHYDROUS $MgWO_4$[a]

High-temperature $MgWO_4$ (*13*)		Dehydration product (this work)	
d	I/I_0	$d_{obs.}$	I/I_0
6.41	36	6.41	53
5.98	14	5.98	16
5.44	14	5.48	9
4.726	23	4.72	55
4.677	20		
4.187	19		
3.772	15	3.79	31
3.589	23	3.62	60
3.361	15		
3.214	100	3.22	100
3.059	24	3.07	33
2.976	8		
2.759	9	2.75	47
2.592	11	2.56	
2.532	12		
2.499	14	diffuse	13
2.445	16	2.46	
2.354	15	2.36	33
2.329	11		
2.296	15		
2.199	2		
2.164	22		
2.137	43	2.14	33
2.078	12	2.08	27
2.045	1		
1.9713	3		
1.9552	3		
1.9355	2		
1.8900	11	1.91	24
1.8489	8		
⋮			

[a] Comparison of literature data (*13*) for "high temperature $MgWO_4$" with the pattern of dehydrated $MgWO_4 \cdot 2H_2O$ and $MgWO_4 \cdot H_2O$ (this work).

in positions reproducible from one pseudomorph to the other, implying topotaxy for the second step of dehydration as well. However, they are so complex that we did not succeed in extracting a meaningful unit cell, most probably because of long axes, low symmetry, and multiple twinning on different planes. We therefore feel that the tetragonal symmetry suggested in (*1*) may be ruled out. Although we thus cannot contribute to the solution of its structure, some observations on the behavior of this phase on further heating may help to improve the understanding of $MgWO_4$ obtained from hydrated precursors, the powder diffraction pattern of which shows broadened reflections, but is surprisingly similar to the pattern reported for the high-temperature form of magnesium tungstate registered at 1200°C (*13*), as shown in Table V.

Differential thermal analysis (DTA) measurements and continuous high-temperature powder diffraction show an endothermal phase transformation into the wolframite type structure to occur at 650°C. This agrees with literature data (*1, 2, 9, 14*), except for the somewhat lower transition temperature found in our work. Above 1200°C, a reversible phase transformation is observed in DTA, but these temperatures have not been accessible for X-ray diffraction in our experiments.

It obviously corresponds to the transformation into the high-temperature form of $MgWO_4$ as reported to occur at 1165°C (*13*). These observations can be explained as follows: $MgWO_4$ exists in two, and only two, modifications, of which the wolframite type is thermodynamically stable below ca. 1200°C. Dehydration of both of the hydrates leads topotactically to metastable high-temperature $MgWO_4$ because of a certain, still unknown structural similarity. At 650°C the activation energy is brought up for transformation into the stable wolframite type. The latter suffers a phase change at around 1200°C, as also reported by other authors. These arguments agree with the fact that the poorly crystalline form of $MgWO_4$ has so far always and only been observed, when the preparation started from hydrated precursors. It does therefore most probably represent a further example of an otherwise unstable crystal

structure at the prevailing temperature, being accessible through a topotactic pathway, a phenomenon for which a number of other cases are known (*24*).

References

1. A. N. Borshch, Yu. G. Dorokhov, and M. V. Mokhosoev, *Russ. J. Inorg. Chem.* **19,** 953 (1974).
2. A. N. Borshch, N. G. Kisel, and A. M. Golub, *Sov. Progr. Chem.* **39,** 1 (1973).
3. J. Ullik, *Sitz. ber. Acad. Wien* **56,** 152 (1867).
4. I. Lefort, *Comptes Rendu* **88,** 798 (1876).
5. A. N. Borshch, M. S. Beginina, N. G. Kisel, and A. M. Golub, *Russ. J. Inorg. Chem.* **18,** 415 (1973).
6. Y.-H. Tsay and J. V. Silverton, *Z. Kristallogr.* **137,** 256 (1973).
7. J. R. Günter, "Reactivity of Solids" (P. Barrett and L.-C. Dufour, eds.), Mat. Sci. Monogr., No. 28 A, p. 485, Elsevier, Amsterdam, 1985; and E. Dubler and J. R. Günter, to be published.
8. J. R. Günter and W. Bensch, to be published.
9. N. J. Dunning and H. D. Megaw, *Trans. Faraday Soc.* **42,** 705 (1946).
10. E. Broch, *Z. Phys. Chem. B* **1,** 409 (1928).
11. *Z. Kristallogr.* (Strukturber Suppl.) **2,** 85 (1928–1932).
12. G. R. Fonda, *J. Phys. Chem.* **48,** 303 (1944).
13. L. L. Y. Chang, M. G. Scroger, and B. Phillips, *J. Am. Ceram. Soc.* **49,** 385 (1966).
14. C. G. A. Hill, *Trans. Faraday Soc.* **42,** 685 (1946).
15. B. A. Frenz, Enraf-Nonius Structure Determination Package. SDP Users Guide, version April 1983.
16. K. Okada and J. Ossaka, *Acta Crystallogr. Sect. B* **36,** 657 (1980).
17. E. Dubler, G. B. Jameson, and Z. Kopajtić, *J. Inorg. Biochem.* **26,** 1 (1986).
18. J. R. Günter, "Reactivity of Solids," (K. Dyrek *et al.*, Eds.), Vol. 2, Mat. Sci. Monogr., No. 10, p. 913, Elsevier, Amsterdam, 1982.
19. R. Schneider, J. R. Günter, and H. R. Oswald, *J. Solid State Chem.* **45,** 112 (1982).
20. J. R. Günter and H. R. Oswald, *Bull. Inst. Chem. Res. Kyoto Univ.* **53,** 249 (1975).
21. J. Y. Le Marouille, O. Bars and D. Grandjean, *Acta Crystallogr. Sect. B* **36,** 2558 (1980).
22. O. Bars, J. Y. Le Marouille, and D. Grandjean, *Acta Crystallogr. Sect. B* **37,** 2148 (1981).
23. O. Bars, J. Y. Le Marouille, and D. Grandjean, *Acta Crystallogr. Sect. B* **37,** 2143 (1981).
24. H. R. Oswald and J. R. Günter, "1976 Crystal Growth and Materials" (E. Kaldis and H. J. Scheel, Eds.), Current Topics in Materials Science, Vol. 2, p. 416, North-Holland, Amsterdam, 1977.